IMAGE QUALITY OF 3.6 m OPTICAL TELESCOPE

Anisha

Panjab University , Chandigarh

Under the supervision of Dr. Brijesh Kumar

Aryabhatta Research Institute of Observational Sciences

Nainital

MAY 27, 2015 - JULY 21, 2015

ACKNOWLEDGEMENT

It has been a great honour and privilege to be selected for the Summer Project at Aryabhatta Research Institute of Observational Sciences through Indian Academy of sciences. I have taken efforts in this project. However, it would not have been possible without the kind support and help of many individuals. I would like to extend my sincere thanks to all of them.

I am highly indebted to Dr. Brijesh Kumar for his guidance and constant supervision as well as for providing necessary information regarding the project and also for his kind support in completing the project.

I would also like to acknowledge my co- summer fellows, Anusree Devanandan and Avni Parmar for helping me with their concepts and suggestions and for keeping my morale high.

Anisha

ABSTRACT

CONTEXT

The 3.6m optical telescope is being installed at Devasthal, Nainital, and it will provide seeing limited observational capabilities at visible and near infrared bands. The image quality of any optical telescope is very crucial to determine accurate physical properties of celestial objects and it can go bad due to variety of reasons and it can go bad due to variety of reasons such as poor alignment of optics and the environment of telescope.

AIM

The aim of the project deals with the detection of wavefront distortion induced by misalignment of optics and other imperfections in telescope using Shack Hartmann wavefront sensor.

METHOD

Using modal wavefront reconstruction approach, the distorted wavefront has been reconstructed for 3.6m telescope in terms of zernike modes and a value of

RESULT

RMS wavefront error of 184nm has been obtained. PSF and MTF of the image are also extracted using these zernike coefficients.

DISCUSSIONS

The values obtained are consistent with the image quality specification of the telescope.These values donot include seeing in then and describe the optics of telescope when installed in space.

INDEX

1. INTRODUCTION

The 3.6m optical telescope is being built at Devasthal, Nainital about 2420m above sea level, with an aim to provide observational facilities at seeing limited imaging capabilities at visible and near infrared bands. It is a two mirror Ritchey Chretien system with both hyperboloidal primary and secondary mirror with f/9 cassegrain focus. It is having alt- azimuth mount with a science field of view of 0.5^{o} and plate scale of 6.4 milliarcseconds per micron. It is equipped with active optics in order to control the optics of system. The performance of the telescope is set to have 80% encircled energy within 0.45 arcseconds diameter.

BASIC ASTRONOMICAL CONCEPTS :

Before dealing with the telescope ,it is important to know about the basic characteristics of astronomical sources. The astronomical sources are defined on a logarithmic scale called magnitude scale.The stars with positive larger value are fainter and with smaller negative value are bright. The relation between apparent flux density and magnitude is as follows :

$$m_1 - m_2 = 2.5 \log \frac{\varphi_2}{\varphi_1} \qquad (1)$$

where φ_1 and φ_2 are the apparent flux densities of two stars with magnitude m_1 and m_2

A no. of factors are taken into consideration at the time of observation of these souces such as selecting region with less zodiacal light and galactic dust , proper choice of time (so that source appears high enough in the sky) in order to maximize sensitivity. The different atmospheric effects are discussed as below:

I. ATMOSPHERIC EXTINCTION:
Due to absorption and scattering of incoming photons with air molecules or dust particles, extinction comes into picture. In absorption , the photon is destroyed and its energy is transferred to molecules like H_2O,CO_2,O_2 which leads to subsequent emission where as in scattering , just the energy and direction of photon is changed.

II. ATMOSPHERIC EMISSION : During day time due to scattering of sunlight and during night, due to airglow and moonlight scattering observations are affected. Thermal emission play its role beyond 2.3μm.

Also the thermal emission by the telescope also prevents the observations beyond 2 μm.

III. ATMOSPHERIC REFRACTION

It is bending of incoming light due to variation of atmospheric density and index of refraction of air with wavelength ,making the source appearing higher in the sky than it is actually The factors affecting this effect are zenith angle, altitude, humidity and wavelength.

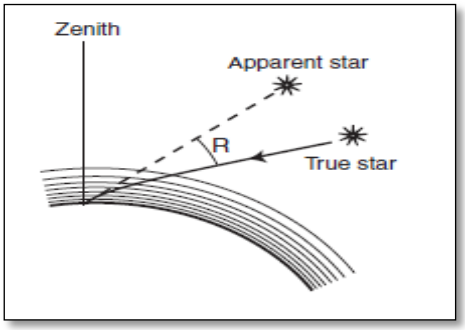

Fig 1: Refraction in the atmosphere of the earth

IV. ATMOSPHERIC TURBULENCE:

The mixing of the layers of the atmosphere with slightly different refractive indexes by wind and convection induces turbulence which change the direction of light passing through, as a result the amount of light entering the aperture of telescope varies constantly in intensity and direction. This phenomenon is called seeing. This is strongly dependent upon the temperature fluctuations which results from turbulent mixing of air layers at different temperatures..The effect of turbulence on optical distortion decreases with the index of refraction of air , which is proportional to density of air , which is further dependent on pressure and inversely proportional to absolute temperature.

The parameters defining seeing are:

FRIED PARAMETER(r_0): It is the diameter of the bundle of rays issued by a source at infinity which travel together through the various turbulent layers and still arrive parallel and in phase at the telescope aperture. The full width at half maximum of the image with aperture greater than r_0 is given as :

$$FWHM = 0.98\frac{\lambda}{r_0} \quad (2)$$

Where λ is the wavelength and $r_0 \propto \lambda^{6/5}$. That further implies seeing varies as $\lambda^{-1/5}$ and thus it is most pronounced at the lower end of optical

range. The image is degraded by the seeing in two ways as image blur and image motion. Small aperture telescope undergoes more image motion than larger telescope due to larger slope changes over wavefront distortion and vice versa for the image blur as can be shown by the figure.

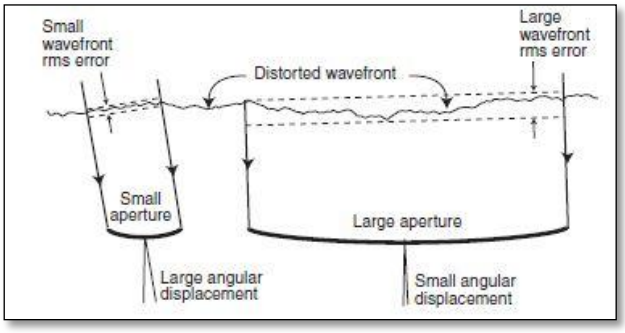

Fig 2: Image motion decreases as telescope size increases where as reverse for image blur

Scintillation is variation in the intensity of image due to curvature of the wavefront over the surface of the aperture which tends to focus or defocus the image and is most effective in small aperture telescope.

V. BACKGROUND SOURCES

Another type of sources that affect observation include natural sources in sky, thermal emission from telescope, side effects in detector itself. These celestial background include galactic background due to dust and faint stars, zodiacal light due to thermal emission from dust grains and scattering from sunlight, degradation of detector pixels due to spurious charges produced by cosmic rays etc. This background fluctuates at the time scale of minutes due to turbulent motion of telescope and temperature variation in telescope.

INSTRUMENTS USED FOR OBSERVATION :

Astronomical observations falls into two categories: imaging, which refers to direct imaging onto detector from telescope and spectroscopy,which refers to production of continuous spectra by means of dispersing element or interferences. In order to serve different purposes, instruments used are camera, photometers, polarimeters and spectrometers. Main detector dealing with the project is CCD.

Charge coupled devices (CCD): It is a two dimensional array of p/n junction made of silicon which is responsible for its response to various wavelengths. The front side of CCD is partially obscured by metal electrodes. Because of this reason it is preferable to illuminate them from rear side which is called backside illumination. In CCD, photoelectrons

produced are stored in the depletion region of the metal insulated semiconductor capacitor, and these stored charges flow from one capacitor to other and further these charge packets(one for each pixel) are detected and measured by the readout electronics(output amplifier). The output voltage signal is converted into digital no. by analog to digital converter. The main characteristics of CCD are :

- CHARGE DIFFUSION: In CCD, voltages are applied in order to hold the charge captured in CCD pixel but it may happen in certain situations that electron moves from its pixel to neighbouring pixel giving rise to phenomenon of charge diffusion.

- CHARGE TRANSFER EFFICIENCY: It is measure of the fraction of charge that is successfully transferred for each pixel transfer. The loss in charge from a CCD pixel containing N electrons that is shifted n times vertically and m times horizontally is given by:

$$L(e) = N(m * CTI(H) + 1024 * CTI(V)$$

- READOUT NOISE: It is the no. of electrons introduced per pixel into final signal upon readout of signal. Binning is done in order to decrease it.

- DARK CURRENT: When the thermal agitation is high enough, electrons will be freed from the valence band and are collected within the potential wall of the pixel and thus contribute to the dark current. It is specified as the no. of thermal electrons generated per second per pixel or actual current generated per area of the device. Therefore, the CCD is operated at very low temperature in order to decrease the dark current either by the use of liquid nitrogen or by some thermoelectric cooling methods.

- CHARGE COLLECTION AND GAIN: Larger the pixel, the more charge can be collected by it. The maximum amount of charge stored by the pixel is termed as full well capacity. The gain determines how the amount of charge in each pixel will correspond to the digital no. in the output image.

- SIGNAL TO NOISE RATIO: The signal S is compared to the fluctuations in the background. Thus the ratio of both comprises the signal to noise ratio which is the strength of measured result expressed in units of standard deviation. S/N for a point or an extended sources covering n pixels on the detector can be expressed as:

$$\frac{S}{N} = \frac{St}{\sqrt{(S + Bn + I_d n)t + {R_n}^2 n + var(B_t nt)}} \qquad (3)$$

where S is the total no. of photoelectrons received from the source per unit time, t is the integration time, B is the no. of photoelectrons received from the background per pixel per unit time , I_d is the dark current of the detector expressed in no. of electrons per pixel and unit time, R_n is the read out noise per pixel(i.e. standard deviation of the readout electrons collected per pixel for each read) and var(B_t n t) is the variance of the total background B_t (B_t = B +I_d +R_n/t) , per pixel per unit time.

2. REFLECTING TELESCOPE OPTICS

2.1. TWO MIRROR SYSTEM:

It is the most widely used configuration because it suffers from minimum reflection and central obstruction losses. It consists of parabolic primary and conical secondary (either ellipsoid or hyperboloid) relaying the common to final focus.

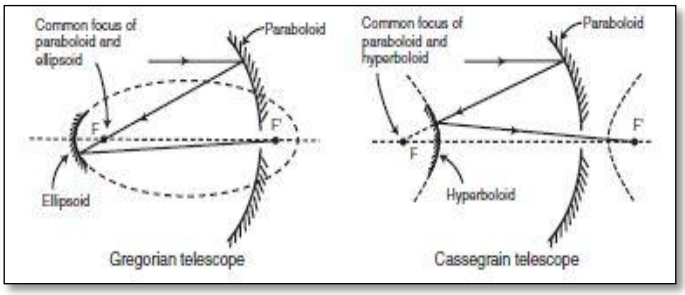

Fig 3: Schematic view of different system of conic surfaces

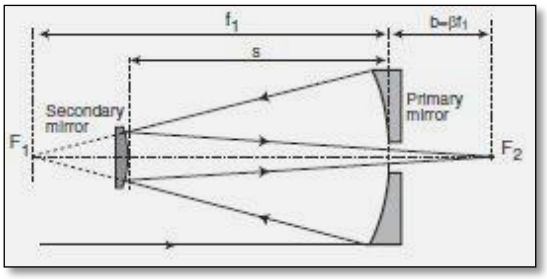

Fig 4: Schematic view of Ritchey-Chretian two mirror system

In addition to these mirrors a no. of other optical elements are added in order to steer the output beam to correct image motion, improving wavefront errors, matching telescope design to detector conditions etc

Some of the basic terms associated with the system is described as below:

- FOCAL RATIO:

$$f\ ratio = N = \frac{f}{D} \qquad (4)$$

where f is the equivalent focal length and D is the diameter of primary mirror. The telescope with large focal ratio are slow and with small ratio are fast.

- PLATE SCALE:

The scale of the image at the focal plane is generally expressed in arcseconds on the sky per millimetre or microns on the image. Being proportional to 1/f , it is given as :

$$Plate\ scale = \frac{206265}{f}\ arcseconds\ per\ mm \qquad (5)$$

- ANGULAR RESOLUTION:

It is the smallest angle between two point sources for which different recognizable images are produced. This is defined relative to Rayleigh criterion which states that the central image of one image falls on the first minimum of the other in order for the two images to be just resolved. Resolving power is inverse of it. The angular resolution $\Delta\theta$ in radians can be described as :

$$\Delta\theta = 1.22\frac{\lambda}{D} \qquad (6)$$

where D is the diameter of the aperture and λ is the wavelength.

There is one more criterion called Sparrow criterion in which resolution limit is defined as the angular separation when the combined pattern of the two sources has no minimum between the centers i.e. when

$$\Delta\theta = \frac{\lambda}{D} \qquad (7)$$

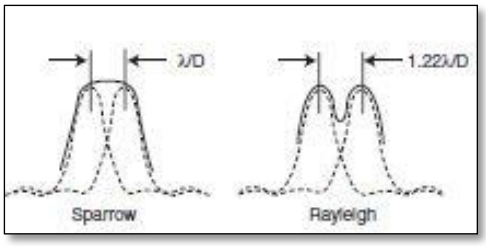

Fig 5: Sparrow and Rayleigh criterion corresponding to separation of λ/D and 1.22λ/D. When the separation of two sources increases the peak of combined pattern first flattens and then there is a dip.

FIELD OF VIEW: The region of the sky visible to a telescope at any one time .It is expressed as :

$$FOV = {Aperture}/{Focal\ length}$$

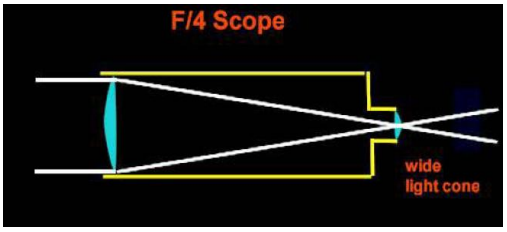

Fig 6:The telescope with wide field of view are slow and with low power small and well suited for viewing many objects at a time like galaxy, clusters etc

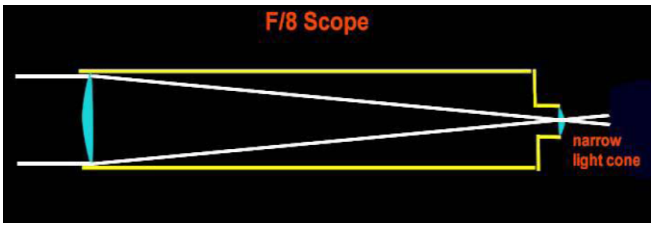

Fig 7: telescope with large focal ratio have narrow FOV with high power and are well suited for stars.

In order to limit the FOV of telescope, field stops are used which limit the extent of the image.

LIGHT GATHERING POWER(A) : Factor representing the photon collection tendency directly dependent upon the field of view.

$$A = T({D}/{S})^2 \quad (8)$$

where D – diameter of the telescope, S - diameter of the pupil of eye

T–Losses due to optics and detector

For 3.6m optical telescope, with focal ratio f/9 and thus effective focal length of 32.4m possess a plate scale of 6.4 milliarcseconds per micron and science field of view of 0.5º. It has a resolution of 38 milliarcseconds and light gathering power of 5.184×10^5 *T.

2.2 PRIMARY ABERRATIONS : Aberrations refer to failure of the optical system to produce an exact point to point correspondence between the source and its image. Chromatic aberration are absent in reflecting system as the laws of reflection are independent of wavelength. There are five primary aberrations of reflecting system which are as follows:

- Spherical aberration(on axis image error) It is the aberration exhibited by spherical mirror imaging a source at infinity i.e. the rays issuing from a source at infinity do not all converge at the same point. The focus of marginal rays are different from the focus of paraxial rays. This is independent of the field angle and inversely proportional to the cube of focal ratio.
- COMA: When the rays from an off axis source do not converge at the same focus in plane, image is blurred. It is field dependent and increases linearly with the off axis angle and is inversely proportional to the square of focal ratio.
- ASTIGMATISM: This error is due to fact that focus of rays in plane containing from axis and an off axis source (tangential plane) is different from the focus of rays in the perpendicular plane(sagittal plane). It varies as square of the field angle and is inversely proportional to f ratio.
- FIELD CURVATURE: In this image is not formed on plane but on curved surface.
- DISTORTION: It occurs because of variation of plate scale with field angle and direction. It scales as cube of field angle.
  In order to describe these image errors mathematically, polynomial representations are used which is described further.

2.3. IMAGE QUALITY OF TELESCOPE

2.3.1 IMAGE FORMATION:

In order to figure out the image quality of optical system, image of point source (stars) is examined. The distribution of light intensity in image of point source is called point spread function. For a perfect optical system, with an unobstructed circular pupil and monochromatic light, the PSF is analytically defined as :

$$I = c\left(\frac{J_{1(x)}}{x}\right)^2, \qquad x = {}^{\pi D\theta}/_{\lambda} \qquad (9)$$

Where I is the intensity of light in the image, C is the constant ,J_1 is the first bessel function with D being the diameter of the aperture , θ being the angular coordinate of the image spread. This is called the airy function. Now, PSF for aperture obstructed at center by the secondary mirror is:

$$I = c\left(\frac{J_{1(x)}}{x} - \varepsilon^2 \frac{J_{1(\varepsilon x)}}{\varepsilon x}\right)^2 \qquad (10)$$

where ε being the obscuration ratio of the telescope expressed as the ratio of the diameter of the central obscuration to that of the aperture. The image is also affected by the diffraction spikes produced by spiders which hold the secondary mirror as these are in incoming beam. Moreover in order to improve torsional stiffness, these vanes are positioned such that these do not converge at the center of gravity and each straight obstruction produces two spikes at 180º apart in direction perpendicular to direction of vane.

2.3.2 CRITERIA FOR IMAGE QUALITY

The image quality is nothing but judging the resolving power of telescope. The factors defining the imaging performance of telescope are other than PSF:

- MODULATION TRANSFER FUNCTION (MTF):

MTF is convolution of the PSF and gaussian image of an object that is continuous sinusoidal intensity pattern i.e. a continuum of dark and bright lines gradually changing from the maxima to minima. Any optical object can be represented as the sum of the infinite series of sinusoidal components of increasing spatial frequency. The MTF is a part of the complex function called Optical transfer function (OTF).

For aberration free aperture , the MTF is given as :

$$MTF(\upsilon) = \frac{2}{\pi}(\varphi - cos\varphi\ sin\varphi), \text{ where}$$

$$\varphi = arccos\frac{\lambda\upsilon}{D}$$

And ν is the spatial frequency(cycles per radian), λ is the wavelength and D is the diameter of the aperture. It takes 0 value at cutoff spatial frequency which corresponds to ultimate resolution of the system λ/D and thus normalised spatial frequency is $\nu_n=\nu/\nu_c$ where ν_c is the cutoff frequency λ/D in angular units and ν_n varies between 0 and 1.MTF is as effective as PSF. It is one dimensional function averaged azimuthally.

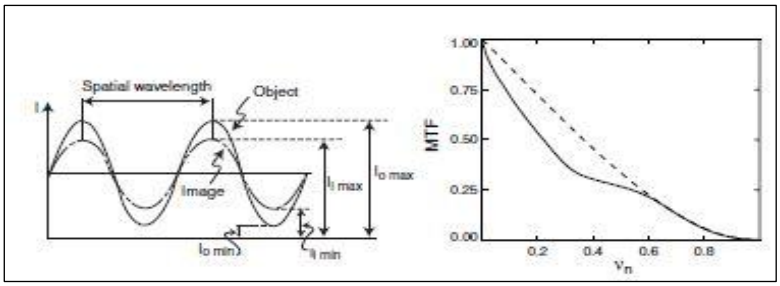

Fig 8:(left) showing sinusoidal component in image with that of object and (right) MTF of aberrated system(solid line) with that of perfect system(dashed line)

- 80% Encircled Energy (EE)

  Fraction of total energy enclosed within a circle of radius centred on the pulse spread function. 80% EE, represents the angular diameter containing 80% of the energy in PSF. For a perfect optical system, this corresponds to be confined within ~ 1.8λ/D. This parameter relates to the sensitivity and angular resolution of telescope. This EE is considered in the range of wavelength from 350nm to 1500 nm.
- FULL WIDTH AT HALF MAXIMA (FWHM): It represents the width of PSF at half the maximum intensity.
- STREHL RATIO:

  It represents the image quality of the system which is close to diffraction limited. It is ratio of the peak intensity in the actual image compared to the peak theoretical diffraction intensity.
- RMS WAVEFRONT ERROR:

  We know that wavefront before entering the system is flat for a source at infinity and when it leaves the system, it is turned into spherical. The deviation of wavefront from a plane or sphere is called waevfront error.

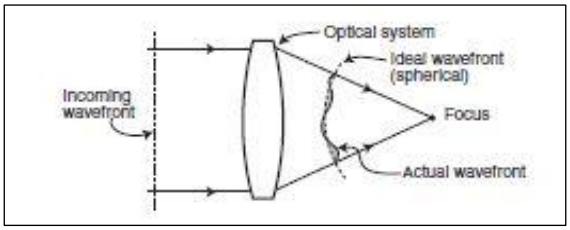

Fig 9 showing schematic view of wavefront propagating through optical system

The magnitude of this error can be expressed as the root mean square of the deviation over the entire surface of

wavefront and is expressed in nanometers or as a fraction of wavelength.

3. ACTIVE OPTICS

Active optics is an approach used to control the optical quality. This automatically corrects the defects in the optics by monitoring the respective positions of individual optical elements and measuring the errors in final wavefront and then correcting these by adjusting the position of optical components at low bandwidth. The main advantages of active optics are correction of residual aberrations primarily spherical aberration, adjustment of conical constant of primary mirror in the sky.

Further using these, effects of atmospheric turbulence can be minimised after the correction of wavefront surface.

3.1. WAVEFRONT SENSORS

These are used for detecting wavefront deformations by sampling wavefront or mirror surface through screens. There are different types of sensors available like Hartmann, Shack Hartmann and curvature sensor serving different purposes. The sensor which is equipped with the 3.6m Devasthal telescope is Shack Hartmann wavefront sensor. There are two of its type installed one is in the Auto Guiding unit and other is test wavefront sensor. The description is as below:

SHACK HARTMANN WAVEFRONT SENSOR:

Shack Hartmann is modification of Hartmann sensor. In SHS, an lenslet array is used which focus telescope entrance pupil on the detector. Since the lenslet array is not perfect, therefore it is first calibrated with reference flat wavefront. With ideal wavefront normal to SHS, well focussed equidistant spots are formed on the CCD placed at the focus of the lenslet array. There is shift in the position of the spots with distorted wavefront which when measured can be used to detect the local slopes of the wavefront.

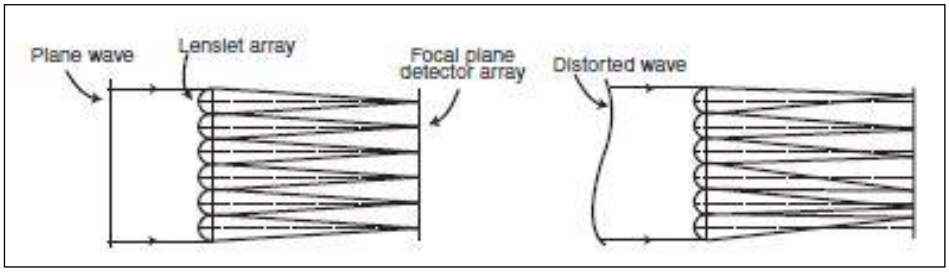

Fig 10: Schematic view of the formationof spots due to plane and distorted wavefront incident on SHS

The sampling interval of wavefront is in order of minute for active optics. The telescope exit pupil of 30 cm is sampled into spots through the square lenslet array. The SHS installed in AGU along with its parameters is described below :

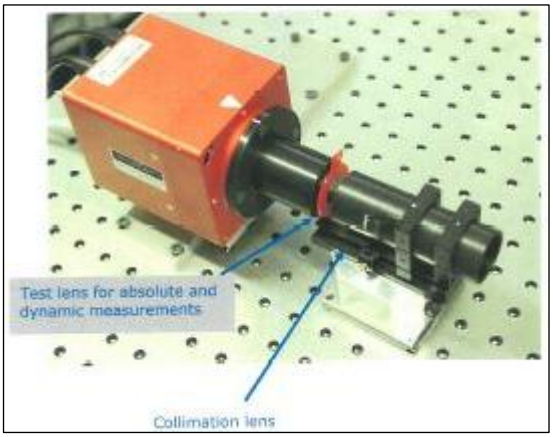

Fig 11 showing the SHS installed in the AGU

Diameter : 1092microns

Focal length: 70mm

Sampling :11×11

Pixel size on CCD detector:13 microns

The diffraction spot size semidiameter ρ is given as:

$$\rho = \frac{f\lambda}{d} \qquad (11)$$

where d and f are the diameter and focal length of the lenslet. The angular dynamic range is defined as the maximum possible angular aberration that can be measured without any crossing or overlapping of spots. Thus the maximum allowed spot deviation is about d/2- ρ so that angular dynamic range becomes

$$\theta_0 = \frac{d/_2 - \rho}{f} \qquad (12)$$

The size σ of each pixel in the detector determines the angular sensitivity, which is the inverse of minimum measurable angular slope:

$$\theta_{min} = \frac{\sigma}{f} \qquad (13)$$

Spot displacement on the detector is equal to the wavefront slope multiplied by the focal length of the lenslet.

4. ZERNIKE POLYNOMIALS

Zernike circle polynomials are basic set of polynomials which are orthogonal over a circle and they are invariant with respect to rotation of coordinate axes about origin. The aberration function of a system with circular pupil can be expanded in terms of these polynomials. Similarly annular polynomials are defined for annular pupil. Any wavefront can be represented as power series expansion of Zernike polynomials as:

$$W(\rho,\theta) = \sum_{n}^{\infty}\sum_{m}^{0} a_{nm} Z_n^m(\rho,\theta)$$

Similar expression also exists in Cartesian coordinates. Zernike polynomials represent balanced aberrations such that a aberration of certain order in pupil coordinates in power series expansion is balanced with aberrations of lower or equal order to minimize its variance. The Zernike expansion coefficient a_{nm} by orthogonality as:

$$a_{nm} = \frac{1}{\pi}\int_0^1\int_0^{2\pi} W(\rho,\theta) Z_n^m(\rho,\theta)\rho\, d\rho d\theta$$

Mean value of aberration

$$\langle W(\rho,\theta)\rangle = \frac{1}{\pi}\int_0^1\int_0^{2\pi} W(\rho,\theta)\rho\, d\rho d\theta$$
$$= 0 for\ n \neq 0, m \neq 0$$
$$= \sum_{n}^{\infty}\sum_{m}^{0} a_{nm}\, for\ n = 0, m = 0$$

Mean square value of aberration and its variance is given as:

$$\langle |W(\rho,\theta)|^2\rangle = \frac{1}{\pi}\int_0^1\int_0^{2\pi} [W(\rho,\theta)]^2\rho\, d\rho d\theta = \sum_{n}^{\infty}\sum_{m}^{0} {a_{nm}}^2$$
$${\sigma_{nm}}^2 = \langle W(\rho,\theta)^2\rangle - \langle W(\rho,\theta)\rangle^2 = a_{nm}^2, n \neq 0, m \neq 0$$

Therefore each expansion coefficient except a_{00} represents the standard deviation of the aberration which only represents the root mean square value of aberration.

$$W_{RMS} = \sqrt{\langle |W(\rho,\theta)|^2\rangle}$$

Further, the standard deviation of any aberration term is equal to the corresponding coefficient a_{nm} because of the orthogonality relation.

5. WAVEFRONT ANALYSIS METHOD

5.1 Acquiring and reducing wavefront sensor data:

We are verifying the image quality of telescope through the WFS in AGU which consists of pick off mirror and a folding mirror to send the source light to guider and SHS. The block diagram of AGU:

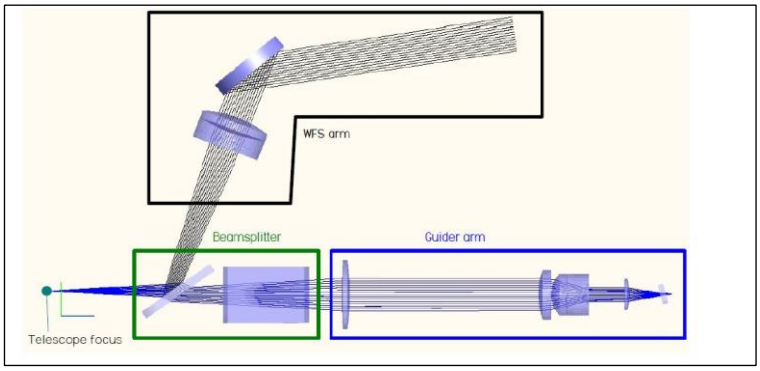

FIG 12: block diagram showing the AGU and WFS

The CCD images are obtained for both distorted wavefront and reference wavefront for a star for a exposure time of 3 seconds which are:

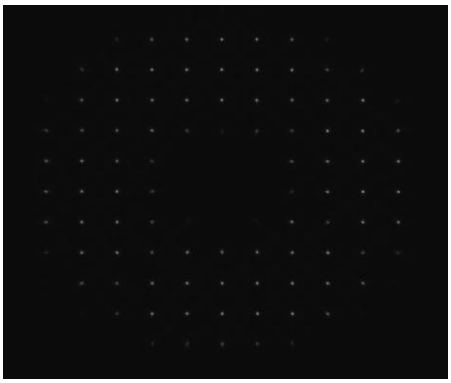

Fig 13: CCD image after sampling of annular pupil

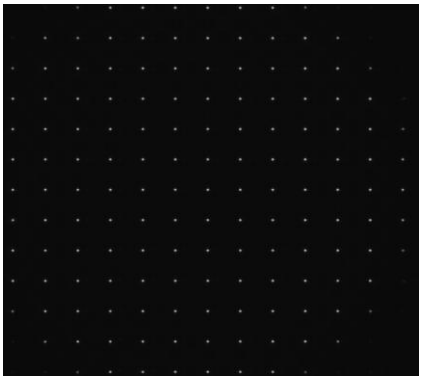

Fig 14: Representative reference image taken with CCD at SHS

In order to calculate the local slope gradient, shift in the spots centres for the perturbed wavefront form reference is calculated using IRAF(image reduction and analysis facility).

Centroiding of the spots is performed using IRAF's DAOPHOT package. The data are initially passed through DAOFIND to locate and identify spots which further involves data acquired through DATAPAR and FINDPAR. After the spot centers for both reference and test image are

obtained, the shift of spots are calculated by the difference of comparable spots.

5.2. Method for reconstruction of wavefront:

Instead of analysing the wavefront through some software, we are doing the same through an adopted method involving Zernike polynomial fitting. This method is called modal approach of wavefront reconstruction

Method description:

In this method, polynomial fitting is used to express the slope deviations which can be performed through least square method. We know that any polynomial can be represented as linear combination of Zernike polynomials as:

$$W(x,y) = \sum_{n=0}^{N} A_n Z_n$$

Where N is the no. of polynomials and A_n are the unknown coefficients to be obtained. Taking the derivative of the wavefront with respect to x and y.

$$\frac{\partial W(x,y)}{\partial x} = \sum_{n=0}^{N} A_n \frac{\partial Z_n}{\partial x}$$

$$\frac{\partial W(x,y)}{\partial y} = \sum_{n=0}^{N} A_n \frac{\partial Z_n}{\partial y}$$

Further it is known that the wavefront deformations are calculated using the spot displacements Δx andΔy from the reference and the focal length of the lenslet array.

$$\frac{\partial W(x,y)}{\partial x} = \frac{\Delta x}{r} = \frac{TA_x}{r}$$

$$\frac{\partial W(x,y)}{\partial y} = \frac{\Delta y}{r} = \frac{TA_y}{r}$$

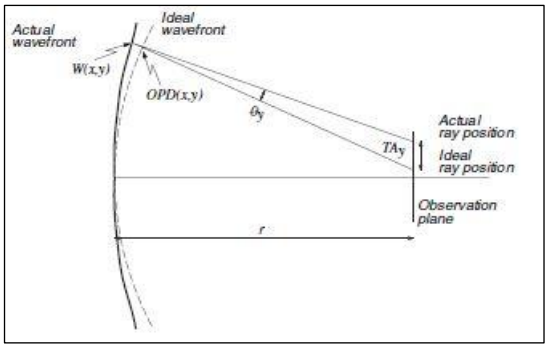

Fig 15: Relation between tranverse aberrations(TA_x,TA_y) and wavefront deformations.

Δx,Δy are calculated by subtracting the coordinates of point corresponding to reference wavefront from the coordinates of points from the wavefront passing through telescope. Then these slope displacements are modelled with 8 term Zernike polynomial fit which represents low order aberrations. The polynomial representations of these aberrations along with their gradients are described in the table1 along their gradients with respect to x and y.

For k no. of spots , these above equation scan be represented in form of array of matrix. Let

$$\frac{\Delta x}{r} = b(x,y) \ , \quad \frac{\Delta y}{r} = c(x,y)$$

$$\frac{\partial W(x,y)}{\partial x} = g(x,y), \frac{\partial W(x,y)}{\partial y} = h(x,y)$$

$$\begin{bmatrix} b(x_1,y_1) \\ b(x_k,y_k) \\ c(x_1,y_1) \\ c(x_k,y_k) \end{bmatrix} = \begin{bmatrix} \begin{pmatrix} g_1(x_1,y_1) & \cdots & g_j(x_1,y_1) \\ \vdots & \ddots & \vdots \\ h_1(x_k,y_k) & \cdots & h_j(x_k,y_k) \end{pmatrix} \end{bmatrix} \begin{bmatrix} A_1 \\ A_2 \\ A_k \end{bmatrix}$$

j represents the no. of modes .

Thus we can write

$$\beta = \alpha\omega$$

Using least squares fitting of the matrices, coefficients can be extracted as:

$$\omega = (\alpha^T\alpha)^{-1}\alpha^T\beta$$

Further we know that these coefficients represent the wavefront error as piston is not included because its derivative is not orthogonal.The total

RMS wavefront error is equal to root of the sum of squares of these modes except piston.

We wrote a code in C++ in order to solve this matrix and a code in order to evaluate the Zernike gradients at different values of x and y.

We applied this modal approach to a set of 82 spots obtained after centroiding and calculated 8 Zernike low order modes which are displayed in the table

Table 1: Representation of Zernike polynomials along with their derivatives

Polynomial	Aberration	W(ρ,θ)	W(x,y)	$\frac{\partial W(x,y)}{\partial x}$	$\frac{\partial W(x,y)}{\partial y}$
Z1	Piston	1	1	0	0
Z2	TiltX	2ρcosθ	2x	2	0
Z3	Tilt Y	2ρsinθ	2y	0	2
Z4	Defocus	$\sqrt{3}(2\rho^2-1)$	$\sqrt{3}(2x^2+2y^2-1)$	$4x\sqrt{3}$	$4y\sqrt{3}$
Z5	Astigmatism X	$\sqrt{6}(\rho^2 cos2\theta)$	$\sqrt{6}(y^2-x^2)$	$-2\sqrt{6}(x)$	$2\sqrt{6}y$
Z6	Astigmatism45	$\sqrt{6}(\rho^2 sin2\theta)$	$2\sqrt{6}(xy)$	$2\sqrt{6}y$	$2\sqrt{6x}$
Z7	Coma X	$\sqrt{8}(3\rho^3-2\rho)cos\theta$	$\sqrt{8}x(3x^2+3y^2-2)$	$\sqrt{8}(9x^2+3y^2-2)$	$6\sqrt{8}xy$
Z8	Coma Y	$\sqrt{8}(3\rho^3-2\rho)sin\theta$	$\sqrt{8}y(3x^2+3y^2-2)$	$6\sqrt{8}xy$	$\sqrt{8}(3x^2+9y^2-2)$
Z9	Spherical aberration	$\sqrt{5}(6\rho^4-6\rho^2+1)$	$\sqrt{5}(6\rho^4-6\rho^2+1)$	$\sqrt{10}(24x^3+24xy^2-12x)$	$\sqrt{10}(24y^3+24yx^2-12y)$

Table 2 showing the Zernike coefficients and final RMS wavefront error in microns

Aberration	Zernike mode
TiltX	-0.149116
TiltY	-0.1078
Defocus	.000102064
Astigmatism X	-1.94×10^{-5}
Astigmatism 45	7.93×10^{-5}
Coma X	2.48×10^{-8}
Coma Y	-2.42×10^{-8}
Spherical Aberration	2.92×10^{-12}
Final RMS error	0.184012

Strehl ratio can be calculated from the RMS wavefront error as:

$$Strehl\ ratio = (e^{-2\pi\omega})^2$$

where ω is the RMS wavefront error expressed in terms of the wavelength. Thus

ω= 184/550 = .334
Strehl ratio = 0.0149

In order to reconstruct the wavefront , we use the graphical user interface developed by James Wyant in web mathematica. We put these coefficients and these generated the wavefront and further the PSF and MTF of the aberration is also generated which are:

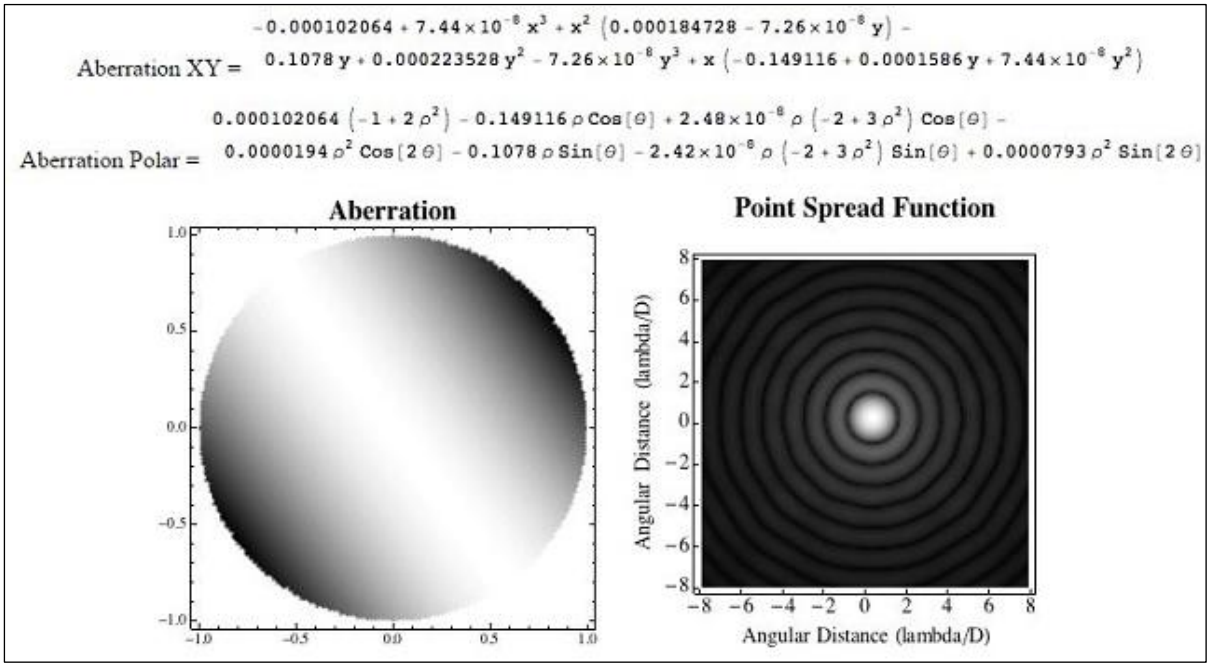

Fig 16: Reconstruction of wavefront and representation of the PSF

The PSF and its fourier transform MTF is as follows:

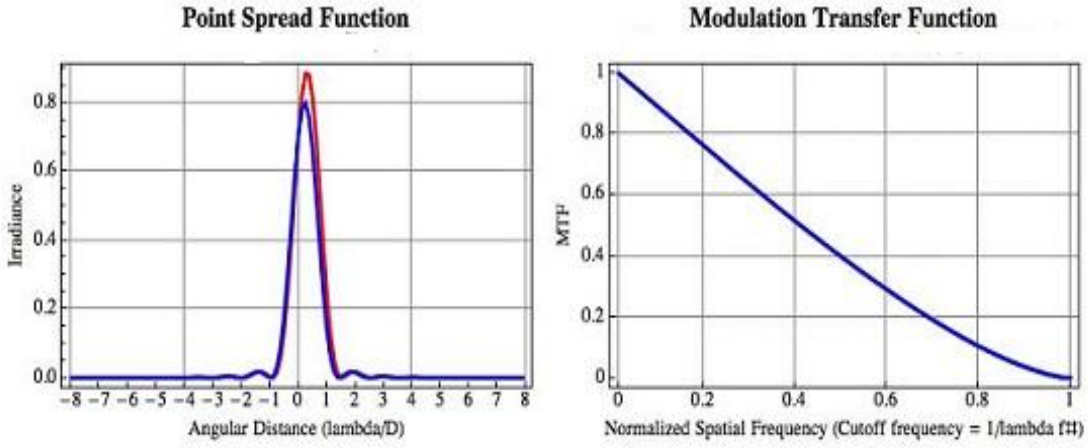

Fig 17: Plot of PSF and MTF

6. DISCUSSIONS:

We obtained an RMS wavefront error of 184 nm for a wavefront distorted by the aberrations caused by optical design. This value was very much in confirmation with value specified. Using the graphical user interface, we reconstructed the wavefront. Further we got the plot of PSF and MTF. In order to calculate the 80%Encircled energy, we used the

Monte Carlo simulated plot of 80% encircled energy for wavelength in the range 350 to 1500 nm vs RMS wavefront error. This Monte Carlo plot is obtained by changing the positions of the mirroe and obtaining the RMS error. The plot is as follows:

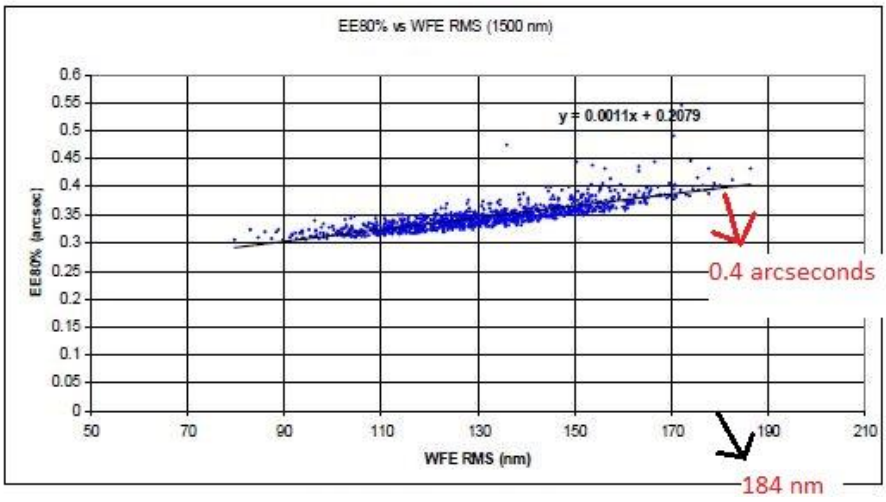

Fig 18 : Monte Carlo simulated plot of 80% EE vs RMS error

Thus for the RMS wavefront of 184 nm , 80% EE is about 0.4 arcseconds. Since there is no chromatic aberration and these aberrations present are only due to the mirrors therefore, there is no wavelength dependence.

Thus the resolution of the image is ~.4 arcseconds and it can resolve only those point sources lying at the angular separation of < 0.4 " otherwise these are unresolved and thus behave as single source.

In this value of resolution, only the diffraction has been taken into effect and seeing is ignored. This can be seen from the 3 seconds exposure time of the images recorded on the CCD during which seeing can be integrated out. Thus the behaviour of the telescope is similar to telescope in space as all the high order aberrations are taken out.

In this project, I went through the optics of the telescope and factors affecting the image formation of the telescope. I studied the principle of SHS and approaches to construct the wavefront from magical Zernike polynomials.

7. FUTURE PROSPECTS

In this project , we did not take into account seeing which is otherwise a very important factor in causing distortion in the wavefront and affecting the image quality of the telescope in ground based telescope. This work can be extended further in order to calculate the seeing at a particular site and thus calculating the total resolution of the telescope. This can be

approached after reconstructing the wavefront imaged on the focal plane of the telescope and thus calculating the PSF . One we have already extracted from the SHS and the difference of both affectly give the seeing at that site.

8. REFERENCES

1. Pierre Y Bely – The design and construction of large optical telescope, 2003 edition , Springer
2. Daniel Malcara – Optical shop testing , Third edition , john Wiley & Sons
3. C R Kitchin – Astrophysical Techniques, Sixth edition , CRC press Taylor and Francis group
4. Notes on Amateur optics telescope
5. T. E Pickering , S C West & D . G . Fabricant , " Active optica and wavefront sensing at the upgraded 6.5 meter MMT"
6. S A Potanin , " Shack hartmann sensor for testing the quality of optics of the 2.5 m SAI Telescope" Astronomy Reports Volume 53, Issue 8 , pp 703-709(2009)
7. Akondi Vyas , M B Roopashree , B Raghvendra Prasad , " Centroid Detection by Gaussian PatternMatching in Adaptive Optics"
8. James C Wyant , "Basic Wavefront Aberration Theory For Optical Metrology"
9. Sopia I. Panagopoulou , Daniel R .Neal, " Zernike vs Zonal Matrix Iterative Wavefront Reconstructor "
10. Patrick Y. Maeda, " Zernike Polynomials and their Use in Describing the Wavefront Aberration of the Human Eye"
11. Steve B. Howell , Handbook of CCD Astronomy, Second edition , Cambridge University Press.